energy&fuels

Article

pubs.acs.org/EF

Hydrate Size Measurements in Anti-agglomeration at High Watercut by New Chemical Formulation

Minwei Sun,[†] Abbas Firoozabadi,*[,†,‡] Guang-Jin Chen,[§] and Chang-Yu Sun[§]

[†]Reservoir Engineering Research Institute, 595 Lytton Avenue, Suite B, Palo Alto, California 94301, United States

[‡]Department of Chemical and Environmental Engineering, Yale University, New Haven, Connecticut 06511, United States

[§]State Key Laboratory of Heavy Oil Processing, China University of Petroleum, Beijing 102249, People's Republic of China

ABSTRACT: Risk management of gas hydrates is a major challenge in offshore hydrocarbon production. Use of anti-agglomerants (AAs) is an attractive option because of effectiveness at low dosage and high subcooling. The literature suggests that anti-agglomeration requires formation of water-in-oil emulsion. Our recent work has demonstrated that the process can occur without emulsion or through oil-in-water emulsion. We have shown anti-agglomeration in oil-free systems in methane hydrates and natural gas hydrates. In this work, through particle size measurements in an autoclave setup in both freshwater and brine, light is shed on the effectiveness of our chemical formulation. Hydrate particle sizes are determined by the focus beam reflectance measurement (FBRM). The results show that our formulation reduces hydrate particle size significantly and eliminates large particles. The AA formulation is a mix of three chemicals: surfactant, base, and oil (e.g., *n*-octane). *n*-Octane helps with even distribution of the surfactant in the solution. The base helps with elimination of small amounts of hydrogen ions in the aqueous solution in conditions when acid gas species are present in the natural gas. These two additives increase the effectiveness of the surfactant for anti-agglomeration. Hydrate particle size measurements show that small amounts of *n*-octane reduce particle sizes by a factor of 2. Our measurements reinforce the idea of effective anti-agglomeration to be the most feasible approach in hydrate flow assurance, with superiority over other alternatives. The formulation has many features, including viscosity reduction of slurry.

INTRODUCTION

Small gas molecules (e.g., methane, ethane, propane, carbon dioxide, and nitrogen) in oil and natural gas flowlines often form gas hydrates with water at low temperature and high pressure.[1−4] Such crystalline complexes raise flow assurance challenges because they may block flowlines and cause serious safety and environmental issues. Hydrate formation resulted in the failure of oil capture from the seabed in the accident in the Gulf of Mexico.[5] The traditional method by thermodynamic inhibitors becomes less attractive in offshore oil/gas operations and productions because of the demand for large quantities of alcohols, e.g., up to 60 wt % in the aqueous phase to shift the equilibrium of the hydrate regime.[3] The alternative approaches rely on changing hydrate surface properties with small chemical quantities, which are referred to as the low-dosage hydrate inhibitors (LDHIs, <2.0 wt %), including kinetic inhibitors (KIs) and anti-agglomerants (AAs).[1,3,6] KIs are generally ineffective at high subcooling (e.g., >10 °C), which is often the case in deepwater. AAs become a promising option because the formation of dispersed small hydrate particles allows for slurry flow.

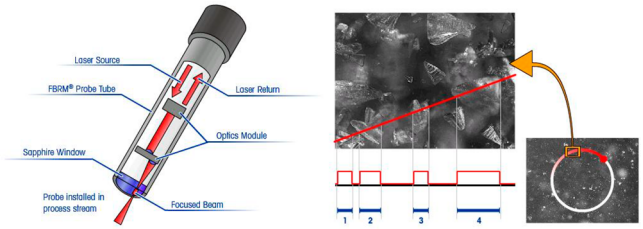

Figure 1. Schematic diagram of the (a) FBRM probe and (b) chord length during in-process measurement (modified with permission from the Mettler Toledo website).

Gas hydrate plugging is closely linked to the viscosity increase from hydrate particle agglomeration.[7−10] In pipelines, hydrate particles stick to each other by capillary forces. These aggregates trap free liquid and gas, which results in an effective volume fraction much higher than the true hydrate volume fraction.[11] The large aggregates give a higher hydrate effective volume fraction than the true hydrate fraction because of liquid entrapment. AAs reduce the capillary forces, leading to a decrease in the effective hydrate volume fraction, resulting in slurry flow without plugging. Hydrate particle size measurements provide basic data to improve the understanding of hydrate slurry rheology and the anti-agglomeration mechanism.

The general belief in the hydrate literature has been that an oil phase in large quantities is required for hydrate anti-agglomeration.[1,12−15] The mixtures of oil/water/surfactant have been thought to form water-in-oil emulsion, from which hydrate particles can be dispersed in the oil phase when the conditions fall into the hydrate regime.[1,3] Our recent work has

Special Issue: 15th International Conference on Petroleum Phase Behavior and Fouling

Received: October 24, 2014
Revised: January 25, 2015
Published: January 26, 2015

DOI: 10.1021/ef502077d
Energy Fuels 2015, 29, 2901−2905

demonstrated that hydrate anti-agglomeration can realize in water-in-oil emulsions, oil-in-water emulsions, and also from micelles in which there is no oil phase in both methane and natural gas systems.[16,17]

Focused beam reflectance measurement (FBRM) is a unique tool to measure particle and droplet sizes in real time. A rotating precision optics focuses a solid-state laser beam at the interface between the probe window and the actual process, as seen in Figure 1a. In this way, the focused beam scans a circular path across the probe window, where individual particles or particle structures will backscatter the laser light to the probe and generate distinct pulses of reflected light. The pulses of backscattered light are detected by the probe and translated into chord lengths based on a simple calculation of the scan speed (velocity) multiplied by the pulse width (time); a chord length is simply defined as the straight-line distance from one edge of a particle or particle structure to another edge, as shown in Figure 1b. The lower limit of sizing measurement is 1 μm in the probe used in this work.

The FBRM probe can provide measurement in opaque or dark media and in dense suspensions. It has been employed to study gas hydrate particles in recent years.[12,18−20] The setup can be assembled into an autoclave to study hydrate formation and agglomeration. Turner et al. reported observation of direct transformation of water droplets to methane hydrates in crude oils.[12] The setup can also be integrated into a flow loop to monitor the flow behavior.

Particle vision and measurement (PVM) is another tool for sizing measurement. It provides the real-time imaging of particles and droplets as they exist in crystallization in a vessel or a pipeline. Sapphire lens allow the probe to work at high-pressure conditions. PVM is especially useful in capturing the images of large particles.

MATERIALS AND METHODS

The sizing measurement experiments are performed in an autoclave apparatus shown in Figure 2. The effective internal volume of the autoclave is 535 mL (51.84 mm in diameter and 320 mm in depth). The water bath jacket is connected to a Huber chiller for temperature control. The stirring speed is set to 350 rpm in all of the tests. A FBRM probe (D600X) and a PVM probe (V700S-5-K), both manufactured by Mettler Toledo, are installed in the system for sizing measurements. The particle sizes are measured right before cooling at 20 °C and at 1 °C when the hydrates are fully developed and steady state is reached. The reactor is loaded with 180 mL of liquid sample, a mixture of the additives, and water or brine (4.0 wt % NaCl), before evacuation. Both probe windows are installed below the liquid level. Then, the reactor is charged with test gas (methane at 80 bar and natural gas with compositions presented in Table 1 at 50 bar) with stirring at 20 °C. After the gas inlet valve is closed, the water bath is kept at 20 °C for 30 min with stirring before being cooled from room temperature to 1 °C at the rate of −4 or −10 °C/h. The temperature is then kept at 1 °C for a period of time, allowing the gas hydrates to further develop before the temperature ramps back to the initial temperature. A sharp pressure change indicates hydrate formation/dissociation.

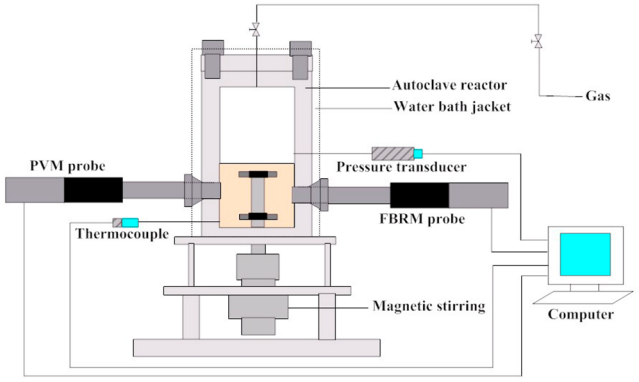

Figure 2. Schematic diagram of the autoclave reactor with FBRM and PVM probes.

The AA (from Lubrizol Corporation) contains 80−89% cocamidopropyl dimethylamine (as the effective component, shown in Figure 3), 5−10% glycerin, and small amounts of free amine and water. Glycerin and small amounts of amine and water are byproducts of surfactant synthesis. Because the concentration of these byproducts is very low (<0.05 wt %), their thermodynamic effect is expected to be negligible.

RESULTS AND DISCUSSION

In this work, we use the autoclave reactor apparatus to form gas hydrates, including methane hydrate [structure I (sI)] and natural gas hydrate [structure II (sII) because of the presence of ethane and propane]. The hydrate particle sizes are measured by the FBRM probe. We investigate the effect of AA dosage, cooling rate, salt, addition of a small amount of oil, and pH adjustment by NaOH on particle size. In the following, we will first present our results in methane hydrates and then in natural gas hydrates.

Methane Hydrate Tests. We first investigate methane hydrates in water without additive. The change of chord length distribution (CLD) is presented in Figure 4a. Ideally, there should be no chord length detected before hydrate formation when there is no surfactant added. However, gas bubbles in the system show a median size of 4.8 μm because of strong stirring. The onset temperature of hydrate formation is in the range of 7.0−9.1 °C, and the onset pressure is in the range of 77−78 bar. The onset temperature is lower for the high rate of cooling. For example, in the blank test, the onset of the hydrate formation temperature is 9.1 °C, where the cooling rate is −4 °C/h. The onset temperature is 7.0 °C in the test of 0.50 wt % AA, and the cooling rate is −10 °C/h. Although we have some duplicate runs, we only report results from single runs. The focus of this work is on the size trends after all hydrates have been formed. The sizes reported here refer to the stable values before the temperature ramping. There is, however, a hydrate particle size change during the cooling process. Table 2 presents details of CLD, including median size, mean size (square weighted), and particle counts in different ranges. The median size of hydrate particles is 19.6 μm measured at 1 °C when there is no AA in the solution. The number of small hydrate particles (<10 μm) is 3241, and the number of large particles is 1869 in the range of 50−150 μm.

Table 1. Composition of Natural Gas (Mole Basis)

component	methane	ethane	propane	*n*-butane	isobutane	nitrogen	carbon dioxide
mol %	80.67	10.20	4.90	0.753	1.53	0.103	1.83

DOI: 10.1021/ef502077d
Energy Fuels 2015, 29, 2901−2905

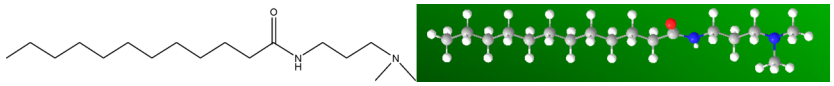

Figure 3. Chemical structures (2D and 3D) of the main component in our AA.

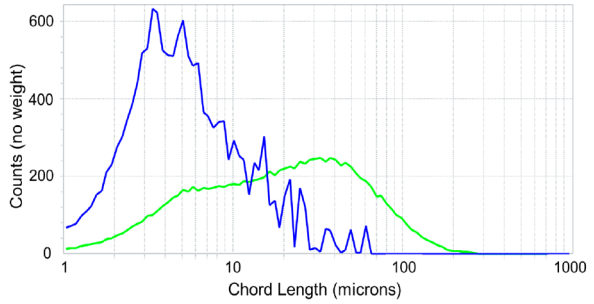

Figure 4. CLD of particles before hydrate formation (blue) and hydrate particles at 1 °C (green, −4 °C/h; red, −10 °C/h) in (a) pure water, (b) 0.2 wt % AA, and (c) 0.5 wt % AA.

Panels b and c of Figures 4 depict the CLD of hydrates in 0.2 and 0.5 wt % AA at different cooling rates (e.g., −4 and −10 °C/h), respectively. The details of CLD are included in Table 2. The weighted mean size of hydrate particles is 47.9 and 49.1 μm in cooling rates of −4 and −10 °C/h, respectively, at 0.2 wt % AA, which are significantly smaller than 100.3 μm in the blank test. When the AA concentration increases to 0.5 wt %, the mean size of the hydrate particles is 32.0 and 32.9 μm in low and high cooling rates. The addition of AA results in a sharp decrease in the size of hydrate particles, as shown in Figure 4 and data in Table 2. For instance, in the range of 50−150 μm, the counts are 1869 without AA and 383 and 198 at the AA dosage of 0.2 and 0.5 wt %, respectively. These sizes correspond to the cooling rate of −4 °C/h. At the same hydrate volume fraction, the mixture with a smaller particle size has lower viscosity.

Figure 5 illustrates an image of a large hydrate particle captured by the PVM probe. The particle size is around 180 μm, and it has an irregular shape, which indicates it is an aggregate of several smaller hydrate particles.

We then investigate the effect of the addition of a small amount of *n*-octane. Oil-in-water emulsions form when 1 vol % *n*-octane is introduced into the aqueous phase with AA. A significant effect of *n*-octane is observed in weighted mean size and the number of large gas bubbles/droplets at the start of the cooling, as shown in Table 3. The number of particles with a size of 50−150 μm decreases from 267 to 13 when *n*-octane is added. The weighted mean size decreases from 28.7 to 19.6 μm, 32% smaller. Because of the much higher solubility of AA molecules in *n*-octane than in water, AA molecules distribute more evenly in water when a small amount of oil is added. As a result, a higher number of AA molecules can bind onto the hydrate particle surface to prevent agglomeration. The weighted mean size of hydrate particles decreases from 32.0 to 21.6 μm at the cooling rate of −4 °C/h and from 32.9 to 30.1 μm at the cooling rate of −10 °C/h. The counts of hydrate particles in the range of 50−150 μm drop from 198 to 14 μm at the low cooling rate and from 362 to 117 μm at the high cooling rate.

The effect of salt addition on the hydrate particle size is also investigated. NaCl brine of 4 wt % is used in place of fresh water to perform the experiments under the same conditions as discussed above. The comparison of the particle size in brine and freshwater is presented in Table 4. The weighted mean size of hydrate particles is 3 times greater in brine than in freshwater (191.3 versus 47.9 μm). The increase is from a large number of particles greater than 50 μm, e.g., 1193 in the range of 50−150 μm and 262 in the range of 150−300 μm. The adsorption of ions on the hydrate particle surface increases the hydrate particle size. We have embarked on molecular dynamics simulations for better understanding of the salt effects at the molecular level. Results will be published in due time. The addition of a small amount of *n*-octane improves the effectiveness of our AA, as indicated by the small number of large particles as Table 4 indicates. In most petroleum fluids, a small amount of hydrocarbon liquids is present, so that there is no need to add *n*-octane.

Natural Gas Hydrate. We also perform four tests in natural gas hydrates. Under test conditions, natural gas forms sII hydrates, different from methane hydrates (sI). We observe foaming as we add AA in the test mixture before hydrate formation; similar observations have been reported in a recent work.[17] The foam increases the gas/liquid interfacial area and reduces the concentration of the surfactant in the aqueous phase. We observe instant plugging from hydrate formation in the natural gas system. The foaming is caused by carbon dioxide in the natural gas, which decreases pH in the aqueous phase, as described by the reaction below.

$$CO_2 + H_2O \rightleftarrows H_2CO_3 \rightleftarrows H^+ + HCO_3^- \rightleftarrows 2H^+ + CO_3^{2-}$$

The molecular structure of AA changes at low pH, and the AA loses effectiveness. To increase the pH of the aqueous phase to a value of above 9, NaOH is introduced into the solution.[17] In

DOI: 10.1021/ef502077d
Energy Fuels 2015, 29, 2901−2905

Table 2. CLD of Particles before Hydrate Formation at 20 °C and Hydrate Particles at 1 °C in Various AA Concentrations at Two Cooling Rates

size and counts	AA = 0%, before	AA = 0%, −4 °C/h	AA = 0.2%, before	AA = 0.2%, −4 °C/h	AA = 0.2%, −10 °C/h	AA = 0.5%, before	AA = 0.5%, −4 °C/h	AA = 0.5%, −10 °C/h
median (μm)	4.8	19.6	4.9	5.7	5.6	5.1	5.4	5.3
mean (square weighted, μm)	29.6	100.3	46.2	47.9	49.1	28.7	32.0	32.9
counts <10 μm	11615	3241	22650	26448	27250	36547	28171	28709
counts 10−50 μm	2808	5082	5474	8919	9053	9956	9379	8949
counts 50−150 μm	102	1869	607	383	351	267	198	362
counts 150−300 μm	0	95	0	3	4	0	0	0

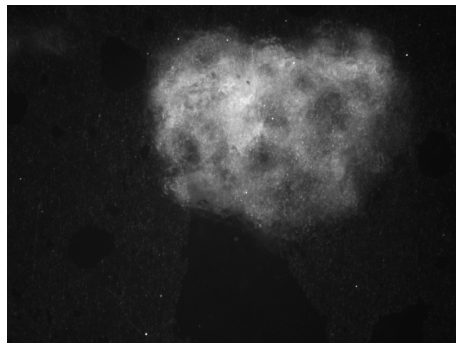

Figure 5. PVM image of the hydrate particle aggregate (180 μm) in the methane hydrate test with no AA.

the autoclave test, the initial pressure of natural gas is 50 bar. The onset temperature of hydrate formation is in a range of 11.1−13.7 °C, and the onset pressure is around 48 bar in the four tests. NaOH at a concentration of 1 wt % is added in the test mixture for pH control. The effect of the AA concentration and addition of a small amount of *n*-octane in the four tests is presented in Table 5. The weighted mean sizes of hydrate particles are 97.1, 48.0, and 38.8 μm at the AA concentrations of 0, 0.2, and 0.5 wt %, respectively, with 1 wt % NaOH and 1 vol % *n*-octane. Without *n*-octane in the mixture, the mean size is almost double (68.7 versus 38.8 μm) in the mixture with 0.5 wt % AA.

There are significantly less large hydrate particles in test 2 than in test 1. The only difference between these two tests is AA dosage, 0% in test 1 and 0.2 wt % in test 2. Possibly there are lots of small particles (<1 μm) in test 2, which are not detected by the FBRM probe because of the resolution of the instrument. We compare the particle sizes in test 2 to the similar test in Table 2 (0.2 wt % AA and −4 °C/h cooling rate). We find that the hydrate particle numbers are 3634 versus 8919 in the range of 10−50 μm and 198 versus 383 in the range of 50−150 μm. The small particle sizes may provide the explanation for the lower viscosity of natural gas hydrates compared to methane hydrates in relation to ball running times in our recent work.[17]

■ CONCLUSION

In this work, we have used FBRM to obtain hydrate particle sizes *in situ* to improve the understanding of the anti-agglomeration mechanism. The results show that our AA formulation can reduce hydrate particle agglomeration significantly in both methane and natural gas systems. We have found that a small amount of *n*-octane reduces hydrate particle size significantly in both freshwater and brine. Hydrate particle size reduction may explain the low viscosity of the hydrate slurries when a small amount of oil, such as *n*-octane, is introduced in the system. The size of the hydrate particles increases with the introduction of 4 wt % NaCl in the aqueous phase. Currently, we are conducting a systemic study on the effects of salt species on hydrate anti-agglomeration and molecular dynamics simulations for an improved understanding. The results will be published as findings are completed.

■ AUTHOR INFORMATION

Corresponding Author

*E-mail: abbas.firoozabadi@yale.edu.

DOI: 10.1021/ef502077d
Energy Fuels 2015, 29, 2901−2905

Table 3. CLD of Particles before Hydrate Formation at 20 °C and Hydrate Particles at 1 °C with 0.5 wt % AA, without and with 1 vol % *n*-Octane (*n*-C_8)

size and counts	without *n*-C_8, before	without *n*-C_8, −4 °C/h	without *n*-C_8, −10 °C/h	with *n*-C_8, before	with *n*-C_8, −4 °C/h	with *n*-C_8, −10 °C/h
median (μm)	5.1	5.4	5.3	5.1	4.8	5.5
mean (square weighted, μm)	28.7	32.0	32.9	19.6	21.6	30.1
counts <10 μm	36547	28171	28709	37088	24017	29538
counts 10−50 μm	9956	9379	8949	8864	5002	9097
counts 50−150 μm	267	198	362	13	14	117
counts 150−300 μm	0	0	0	0	0	2

Table 4. CLD of Methane Hydrate Particles at 1 °C with 0.2 wt % AA in Freshwater and 4 wt % NaCl Brine[a]

size and counts	0.2% AA in freshwater	0.2% AA in brine	0.2% AA with *n*-C_8 in brine
median (μm)	5.7	5.3	5.7
mean (square weighted, μm)	47.9	191.3	138.8
counts <10 μm	26448	18902	30915
counts 10−50 μm	8919	5169	10082
counts 50−150 μm	383	1193	67
counts 150−300 μm	3	262	11

[a]The cooling rate is −4 °C/h.

Table 5. CLD of Hydrate Particles at 1 °C in Natural Gas at a Cooling Rate of −4 °C/h

size and counts	test 1[a]	test 2[b]	test 3[c]	test 4[d]
median (μm)	6.1	5.7	9.3	5.9
mean (square weighted, μm)	97.1	48.0	68.7	38.8
counts <10 μm	22342	9655	14320	14145
counts 10−50 μm	9137	3634	11227	5613
counts 50−150 μm	1198	198	1863	241
counts 150−300 μm	91	2	29	0

[a]Test 1: 0% AA, 1 wt % NaOH, and 1 vol % *n*-octane. [b]Test 2: 0.2 wt % AA, 1 wt % NaOH, and 1 vol % *n*-octane. [c]Test 3: 0.5 wt % AA and 1 wt % NaOH. [d]Test 4: 0.5 wt % AA, 1 wt % NaOH, and 1 vol % *n*-octane.

Notes

The authors declare no competing financial interest.

■ ACKNOWLEDGMENTS

The authors thank the member companies of the Reservoir Engineering Research Institute (RERI) for their financial support. The authors also thank Dr. Jun Chen at the China University of Petroleum for help with the operation on the autoclave reactor.

■ REFERENCES

(1) Sloan, E. D.; Koh, C. A. *Clathrate Hydrates of Natural Gases*; CRC Press: Boca Raton, FL, 2008.
(2) Koh, C. A.; Westacott, R. E.; Zhang, W.; Hirachand, K.; Creek, J. L.; Soper, A. K. *Fluid Phase Equilib.* **2002**, *194*, 143.
(3) Kelland, M. A. *Energy Fuels* **2006**, *20*, 825.
(4) Wu, M.; Wang, S.; Liu, H. *J. Nat. Gas Chem.* **2007**, *16*, 81.
(5) Graham, B.; Reilly, W. K.; Beinecke, F.; Boesch, D. F.; Garcia, T. D.; Murray, C. A.; Ulmer, F. *Deep Water: The Gulf Oil Disaster and the Future of Offshore Drilling (Report to the President)*; United States Government Publishing Office: Washington, D.C., 2011.
(6) Mokhatab, S.; Wilkens, R. J.; Leontaritis, K. J. *Energy Sources, Part A* **2007**, *29*, 39.
(7) Filippov, A. V.; Zurita, M.; Rosner, D. E. *J. Colloid Interface Sci.* **2000**, *229*, 261.
(8) Austvik, T.; Li, X.; Gjertsen, L. H. *Ann. N. Y. Acad. Sci.* **2000**, *912*, 294.
(9) Colombel, E.; Gateau, P.; Barre, L.; Gruy, F.; Palermo, T. *Oil Gas Sci. Technol.* **2009**, *64*, 629.
(10) Moradpour, H.; Chapoy, A.; Tohidi, B. Transportability of hydrate particles at high water cut systems and optimisation of anti-agglomerant concentration. *Proceedings of the 7th International Conference on Gas Hydrates*; Edinburgh, U.K., July 17−21, 2011.
(11) Camargo, R.; Palermo, T. Rheological properties of hydrate suspensions in an asphaltenic crude oil. *Proceedings of the 4th International Conference on Gas Hydrates*; Yokohama, Japan, May 19−23, 2002.
(12) Turner, D. J.; Miller, K. T.; Sloan, E. D. *Chem. Eng. Sci.* **2009**, *64*, 5066.
(13) Mehta, A. P.; Hebert, P. B.; Cadena, E. R.; Weatherman, J. P. *SPE Prod. Facil.* **2003**, *18*, 73.
(14) Sloan, E. D. *Fluid Phase Equilib.* **2005**, *228*, 67.
(15) Zanota, M. L.; Dicharry, C.; Graciaa, A. *Energy Fuels* **2005**, *19*, 584.
(16) Sun, M.; Firoozabadi, A. *J. Colloid Interface Sci.* **2013**, *402*, 312.
(17) Sun, M.; Firoozabadi, A. *Energy Fuels* **2014**, *28*, 1890.
(18) Turner, D. J.; Miller, K. T.; Dendy Sloan, E. *Chem. Eng. Sci.* **2009**, *64*, 3996.
(19) Cameirao, A.; Le Ba, H.; Darbouret, M.; Herri, J. M.; Peytavy, J. L.; Glenat, P. *J. Cryst. Growth* **2010**, *342*, 65.
(20) Leba, H.; Cameirao, A.; Herri, J.-M.; Darbouret, M.; Peytavy, J.-L.; Glenat, P. *Chem. Eng. Sci.* **2012**, *65*, 1185.

DOI: 10.1021/ef502077d
Energy Fuels 2015, 29, 2901−2905